DOI: 10.5604/01.3001.0055.4368
Volume 131 • Issue 1 • July 2025
Journal of Achievements in Materials and Manufacturing Engineering
International Scientific Journal published monthly by the World Academy of Materials and Manufacturing Engineering

Influence of interface notch geometry on the tensile behaviour of FGF-printed parts

M. Shokrollahi [a], A.W. Smith [a], M. Dubé [a,b], I. Tabiai [a,b,*]
[a] Department of Mechanical Engineering, École de Technologie Supérieure, Montréal, Canada
[b] CREPEC, Research Center for High Performance Polymer and Composite Systems, Montréal, Canada
* Corresponding e-mail address: ilyass.tabiai@etsmtl.ca
ORCID identifier: https://orcid.org/0009-0003-4002-9174 (M.S.)

ABSTRACT

Purpose: The paper investigates the influence of interface notches - formed due to extrudate geometry - on the tensile performance of parts manufactured by fused granular fabrication (FGF). Although FGF enables fast, cost-effective, large-scale printing with thermoplastic pellets, its adoption in industry remains limited, mainly due to poor mechanical performance. Interface notches have been identified as a key contributor to this limitation. The study investigates the effect of layer height on notch severity and its impact on the tensile behaviour of PETG samples, to improve understanding and guide process optimisation.

Design/methodology/approach: Single-extrudate-thick PETG walls were printed at two different layer heights (3 mm and 4.5 mm) using a large-scale pellet-fed 3D printer. Tensile specimens were extracted from these walls and tested using digital image correlation (DIC) to map full-field strain. Interface notch geometry was characterised through optical microscopy and image analysis, focusing on key parameters including notch depth, angle, and root radius. The geometric features were then correlated with the tensile properties and localised strain distribution observed during loading.

Findings: Increasing the layer height resulted in deeper, sharper interface notches that raised the strain concentration factor and caused more premature failure. The 4.5 mm layer height sample showed a 31% reduction in ultimate stress and a 29% decrease in strain at break compared to the 3 mm sample. DIC analysis confirmed that the strain localised at the notch roots, highlighting the impact of severe notches on tensile performance.

Research limitations/implications: Future studies could expand on this work by exploring a wider range of layer heights, nozzle sizes, materials, and interfacial healing conditions. Quantifying the evolution of notch geometry across multiple process variables could help establish predictive models for failure.

Practical implications: Understanding the role of notch geometry in FGF-printed parts helps inform optimal printing strategies for improving part strength and reliability. Findings can guide design choices in the structural applications of large-format printing, where the extrudate shape has a significant influence on performance.

Originality/value: The paper highlights the often overlooked role of interface notch geometry as a key driver of failure in FGF-printed structures. By combining DIC and quantitative notch characterisation, it offers new insights into the geometric mechanisms behind anisotropy and strength reduction in material extrusion additive manufacturing.

Keywords: Fused granular fabrication, Interface notch, Digital image correlation, Strain concentration, Tensile properties

Reference to this paper should be given in the following way:
M. Shokrollahi, A.W. Smith, M. Dubé, I. Tabiai, Influence of interface notch geometry on the tensile behaviour of FGF-printed parts, Journal of Achievements in Materials and Manufacturing Engineering 131/1 (2025) 17-25. DOI: https://doi.org/10.5604/01.3001.0055.4368

1. Introduction

Material extrusion additive manufacturing is a 3D fabrication process that utilises a nozzle to extrude and deposit material layer by layer. Fused filament fabrication (FFF) and fused granular fabrication (FGF) are the two technologies within this family which use thermoplastics as the feedstock. In FFF, raw plastic pellets are transformed into filaments and used as input material. The printer used in FGF, on the other hand, employs a screw mechanism inside a barrel to feed, transport and melt the material before extruding it through the nozzle on the platform [1-3]. While FFF is used to print complex geometries with a high overall quality and good surface finish, pellet extrusion printers offer lower costs and are used in various industries to print large parts with specialised materials. The attainable print speed in FGF is also faster due to the use of larger nozzle sizes and higher flow rates. Although FGF achieves higher deposition rates, studies have shown that the tensile properties of FGF parts are generally comparable to those of FFF parts [4], with the final performance in both processes strongly governed by printing parameters and specimen configuration. Moreover, there is the possibility to use recycled materials in FGF by minimising the number of extrusion and melting cycles by directly feeding pellets into the printer [5]. Recent studies have integrated FFF and FGF into single hybrid systems, combining the high detail and surface quality with the high flow rates and material flexibility of pellet extrusion. The setups enhance multi-material and multi-colour printing, optimise the fabrication of large parts, and highlight the growing industrial interest in pellet-extrusion platforms [6,7].

In both methods, deposited filaments weld together and solidify to form a layer and successive layers are extruded on top of each other to complete the final part. Despite their rapid adoption, polymer extrusion methods have seen limited use in high-quality applications due to inferior mechanical performance compared to traditional manufacturing [8-11]. Unlocking such applications requires a deeper understanding of the strength reduction mechanisms in FFF/FGF parts, as schematically illustrated in Figure 1. The first mechanism involves the poor bond formation between consecutive layers of material. Due to rapid cooling of the extrudate during additive manufacturing and low interlayer pressure, achieving a fully formed bond is often hindered [12-16]. The other two mechanisms involve the geometry of the extrudate, which typically has a rounded rectangular shape. It results in a ridge effect on the surface of the printed part and large internal macrovoids, which significantly contribute to the reduction in strength observed in FFF and FGF parts.

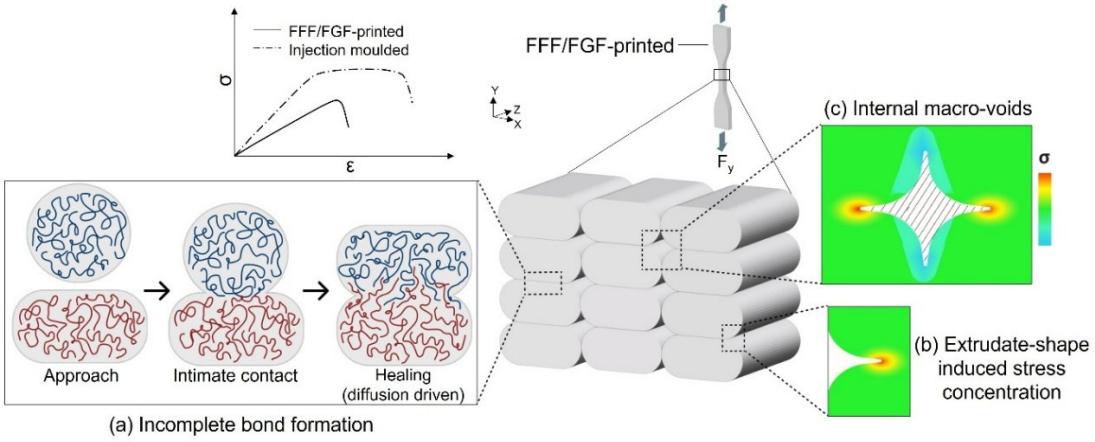

Fig. 1. Schematic of the main strength reduction mechanisms in FFF/FGF printed parts: a) fast cooling of the extrudates prevents the complete interdiffusion of the polymer chains at the interface; b) interface notches act as stress concentration areas; c) porous mesostructure is also a result of the oval shape geometry of the extrudate

Additionally, stress concentration occurs in the valleys formed between adjacent extrudates – referred to as interface notches (see Fig. 1b) – when subjected to loads perpendicular to the print direction [17]. Failure mechanisms in FFF/FGF-printed parts are often linked to mesoscale features, particularly at the level of individual extrudates. Studies have shown that localised strain concentrations at voids and extrudate intersections play a crucial role in progressive failure [18]. While most research focuses on mesostructured features, less attention has been given to extrudate-scale phenomena caused by its shape. A few studies have investigated strain fields around extrudate shape characteristics, revealing that transverse samples – where the load is applied perpendicular to the extrudate direction – fail at lower nominal strain due to local strain concentration at interface notches [19-21]. Kundurthi [22] further quantified the role of notch geometry, identifying notch depth and root radius as key parameters influencing stress concentration.

While previous studies have demonstrated the significant impact of the interface notches on mechanical properties through mechanical testing and FEA, the relationship between the notch severity and print conditions is not well understood, making it difficult to identify optimal printing parameters. Furthermore, prior research has primarily focused on desktop-scale printed parts, with large-scale structures remaining largely unexplored. In this context, FGF was deliberately chosen. Although FDM printers offer greater flexibility in print parameters, FGF is highly relevant for large-scale applications and provides an effective platform for studying interlayer bonding, as the interface formation mechanisms are the same as those in FDM but occur at a larger scale. In this study, Polyethylene terephthalate glycol (PETG) is used to investigate the effects of layer height on interface notch characteristics and the resulting tensile behaviour of FGF-printed samples. The primary objective is to examine how filament geometry and interface notches influence interlayer bonding and tensile performance, rather than to optimise overall specimen strength.

2. Materials and methods

2.1. Printing and sample extraction

PETG pellets were obtained from 3DXTech Advanced Materials, featuring a density of 1.24 g/cc, a glass transition temperature of 80°C measured by differential scanning calorimetry (DSC), and a tensile strength of 45 MPa according to ISO 527 (obtained from the material's datasheet). An AM Flexbot 3D printer, produced by the CEAD company, was used for large-scale printing (Fig. 2). The robot extruder features a base unit that controls temperature, extrusion speed, and automatic material transport. The printer processes various thermoplastic pellets, including short fibre-reinforced ones. Additionally, it features a pellet dryer and a specialised print bed with diversion plugs to enhance workflow efficiency. PETG pellets were used to print a single-extrudate-thick wall, measuring 50 cm in length and 30 cm in height, with a total of 67 layers. One wall was printed for each layer height, following the parameters in Table 1. Direct printing of tensile samples was avoided due to the limited dimensional accuracy of the large nozzle and the asymmetry caused by contact with the bed. Instead, tensile samples (type III) were extracted from the printed walls through CNC milling. Layer heights of 3 mm and 4.5 mm were selected, as they fall within the acceptable range for a 12 mm nozzle, as specified by the printer manufacturer, and yield good print quality on the printed walls.

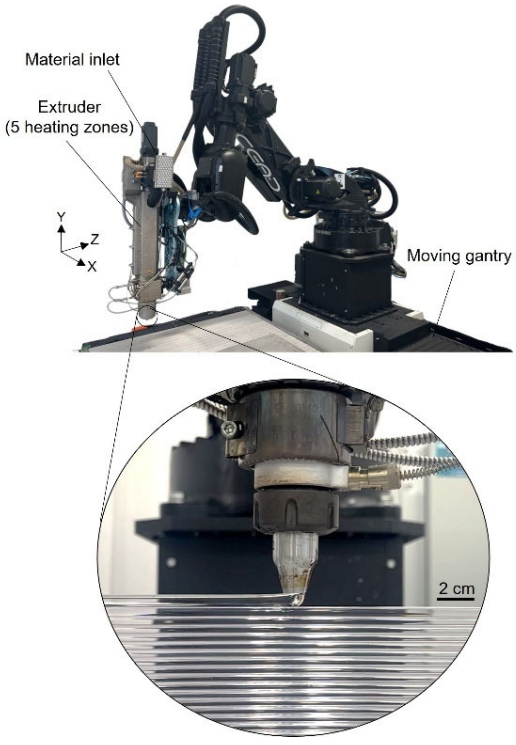

Fig. 2. The robot extruder used for large-scale printing. The zoomed-in view shows the wall being printed

Samples extracted from the wall printed with a 3 mm layer height are labelled LH-3, while those from the 4.5 mm layer height wall are labelled LH-4.5. The schematic illustration of the sample extraction is provided in Figure 3.

Table 1.
Printing parameters

Extrusion temperature, °C	Nozzle diameter, mm	Layer time, s	Layer height, mm	Bed temperature, °C
190-215	12	125	3, 4.5	25

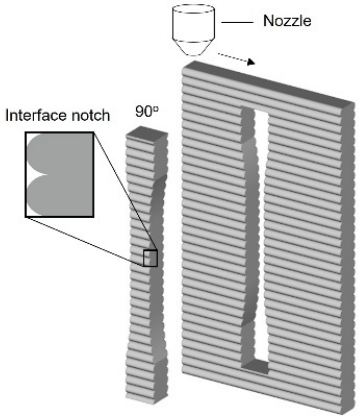

Fig. 3. Schematic illustration of tensile samples extracted from the wall

2.2. Tensile testing

The tensile properties of the samples were determined using an MTS Alliance RF/200 machine equipped with a 200 kN load cell. The samples were pre-conditioned at 60°C for 8 hours before testing. The experiments were performed at a strain rate of 1 mm/mm/min at room environmental conditions. A mechanical extensometer was utilised to measure the sample strain during the test. For the DIC analysis, the virtual extensometer feature in VIC2D was used to calculate the average strain value between two selected points in the gauge length, which is then reported as the nominal strain value. Six samples per set were tested.

2.3. Digital image correlation

A layer of white acrylic colour paint (Vallejo Game Colour) was initially applied to the samples using an airbrush equipped with a 0.5 mm nozzle. Subsequently, the speckle pattern was achieved using a 0.2 mm nozzle to disperse black dots on the white background. The imaging setup utilised a monochrome Grasshopper 3-51SM5M camera carefully positioned for full-field capture during tensile testing. DIC analysis was performed using the commercial software package VIC2D. The smallest subset size was chosen to accurately capture the interfaces, ensuring at least three subsets per layer. Table 2 lists the main DIC parameters, including subset size, step size, and correlation type. Step size refers to the spacing between analysed points. A subset of 2 means that every second pixel is tracked, with the displacements of untracked pixels interpolated. Lagrangian strains were calculated using a 15-pixel filter size. The spatial resolution of displacement measurements (S_{rd}), defined as the distance between independent displacement measurements, is equivalent to the subset size. The spatial resolution of strain measurements ($S_{r\varepsilon}$), or the effective strain gauge length, was computed as: Step × (Strain Filter - 1) + Subset [23]. The speckle pattern and software parameters were optimised to achieve a minimal sigma parameter, which represents the standard deviation of the displacement error, keeping it below 0.03 to ensure low uncertainty.

2.4. Microscopy

Cross-sections of the printed walls were examined under a microscope before the surface machining process. The cut surfaces were polished sequentially with sandpapers of 600, 800, 1200, and 2000 grit to obtain a smooth surface for the optical observations. The observations were performed using a Clemex microscope, and pictures were analysed using ImageJ software to characterise the interface notches, specifically the notch angle, notch depth and notch root radius.

3. Results and discussion

The stress-strain curves, along with the corresponding DIC analysis at different stages of the mechanical tests for LH-3 and LH-4.5, are presented in Figure 4. Nominal stress values were calculated by dividing the load values by the cross-sectional area at the bond width. Nominal strain ($\varepsilon_{yy\text{-}n}$) values are obtained through DIC using a virtual extensometer along the entire gauge length. The stress-strain curves indicate brittle fracture, which may be attributed to strain concentration at the interfaces. DIC results reveal elevated strain values at the interfaces, while significantly lower strain levels are observed between them. The interface regions act as strain concentration zones, which can potentially initiate failure. For LH-4.5, the strain values at the interface before failure are lower, suggesting a higher local strain concentration factor at the interface notch root, which could lead to more premature failure. In contrast, for LH-3, the interfaces experience a higher overall strain level before failure, with the high-strain region being more spread out.

Table 2.
Imaging and DIC analysis parameters

Frame per second	Scale, px/μm	Subset, px × px	Step, px	Correlation type	S_{rd}, mm	S_{re}, mm	Strain variation, %
14	56.8	25	2	Direct	1.42	1.45	0.02

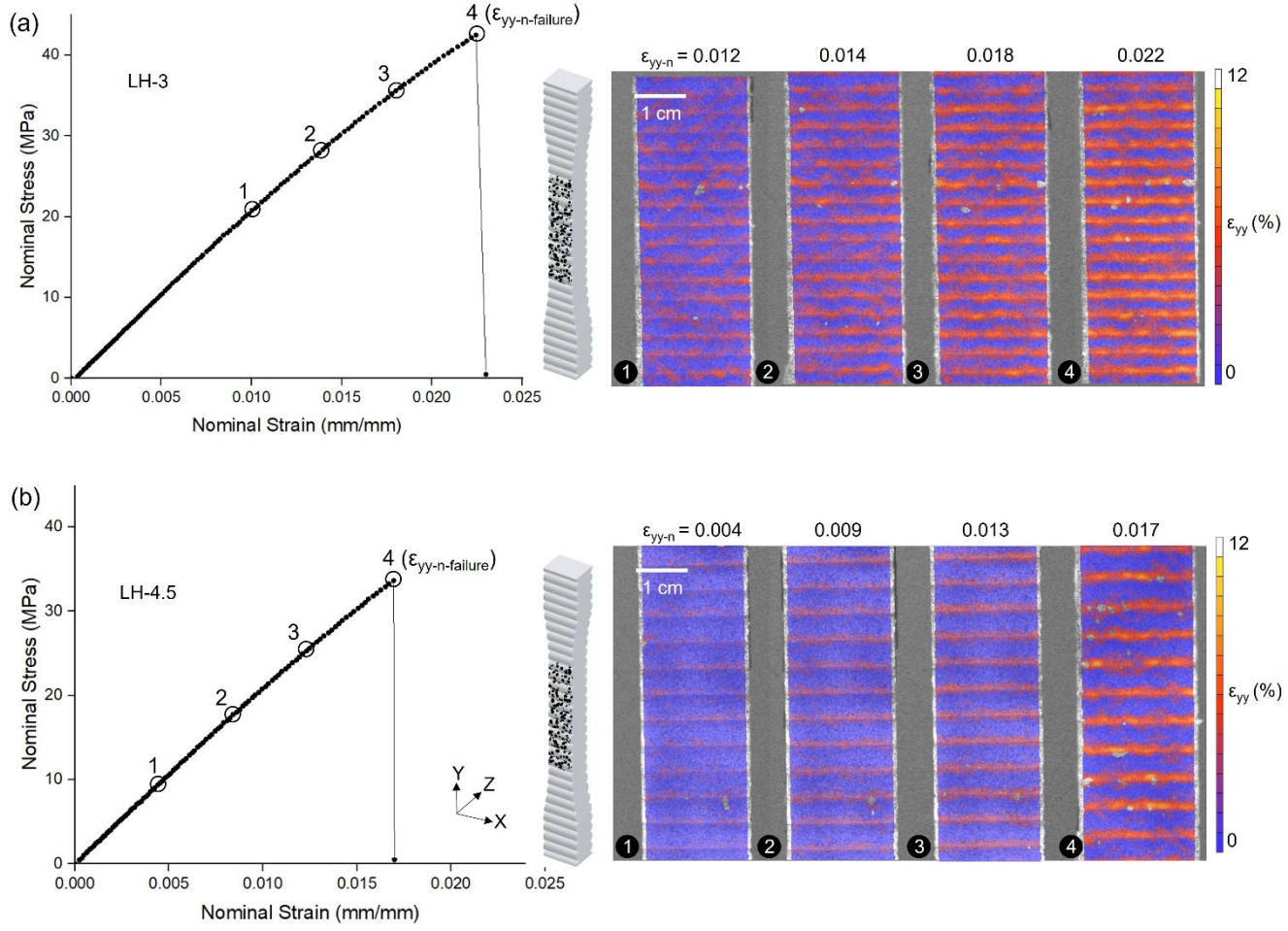

Fig. 4. Stress-strain curve and DIC analysis of a) LH-3 and b) LH-4.5 at various stages. Both samples show a brittle failure, attributed to the premature growth of the crack due to the strain concentration at the interface notches naturally formed during printing

Figure 5a shows DIC results at nominal strain just before failure, highlighting strain concentration at interface notches. The magnified view reveals localised, half-oval-shaped strain fields extending from the notches, with angled high-strain bands. The feature consistently appears across multiple notches, with high-strain regions spanning several millimetres and linking neighbouring notches. Additionally, a high-strain band at a 21° angle suggests that the sample would have likely yielded there if there had been no strain concentration at the edges. Figure 5b displays the strain concentration factor along the z-axis, showing strain localisation within a narrow zone (< 2 mm) that drops off sharply outside it.

According to the results presented in Figure 6, the ultimate stress and strain at break decrease by 31% and 29%, respectively, on average for LH-4.5 compared to LH-3. Kundurthi et al. [22] reported a similar effect, showing a comparable trend with layer height in medium-scale FGF-

printed samples. Allum et al. [20] found that while notches do not affect strength in FFF-printed samples, the strain at break significantly decreases. The results presented here suggest that the local strain concentration effect at the notches intensifies with increasing layer height, resulting in a reduction in the mechanical performance of the parts.

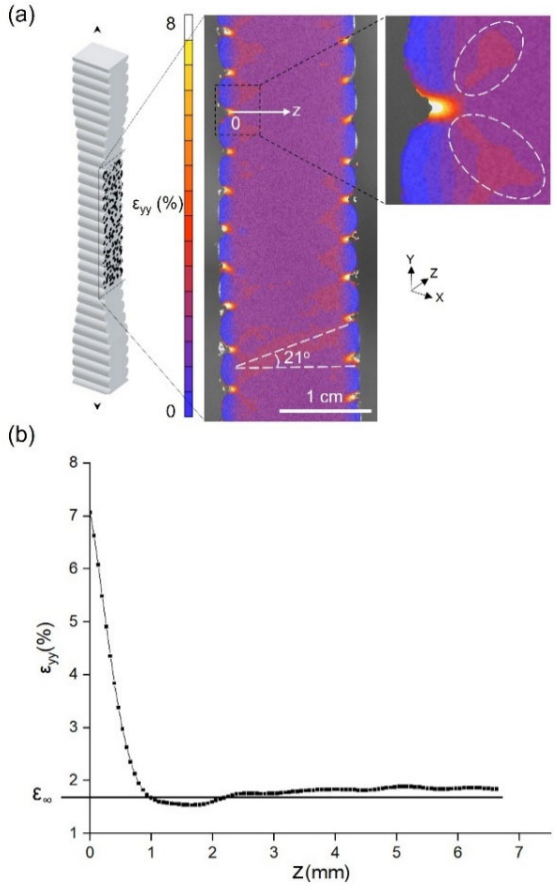

Fig. 5. High-resolution DIC analysis of the LH-4.5 side view at nominal strain before failure reveals localised strain fields caused by interface notches. The fields remain confined to the notch region, with minimal influence beyond. The angled high-strain zone suggests a potential yielding path in the absence of notch-induced concentration

The notch angle characterises the interface notches in both cases (θ), notch depth (a), and notch root radius (r) reported in Table 3. The parameters are schematically shown in Fig. 7. To measure θ, two circles are fitted to the curved openings of the notch angle, and tangents are drawn at their intersections. The angle between these tangents is considered as θ. For the notch root radius, a circle is fitted to the curved root of the notch using the Contact Angle plugin in ImageJ, and the radius of this circle represents the notch root radius. The cross-sectional view of LH-3 shows a U-notch with a curved root, while LH-4.5 displays a V-notch at the interface. The notch root for LH-4.5 is significantly sharper, which could lead to a higher local strain concentration factor. Additionally, a increases while θ decreases, indicating the formation of a more severe notch as the layer height increases.

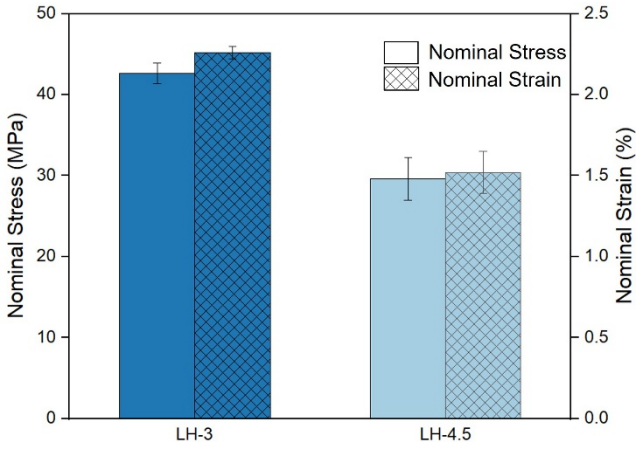

Fig. 6. Ultimate stress and strain at break for LH-3 (42.7 MPa, 95% CI: 42.0–43.4; 2.3%, 95% CI: 2.2–2.3) and LH-4.5 (29.6 MPa, 95% CI: 27.0–32.3; 1.5%, 95% CI: 1.4–1.6). Both values decrease with increasing layer height. Error bars indicate standard deviation

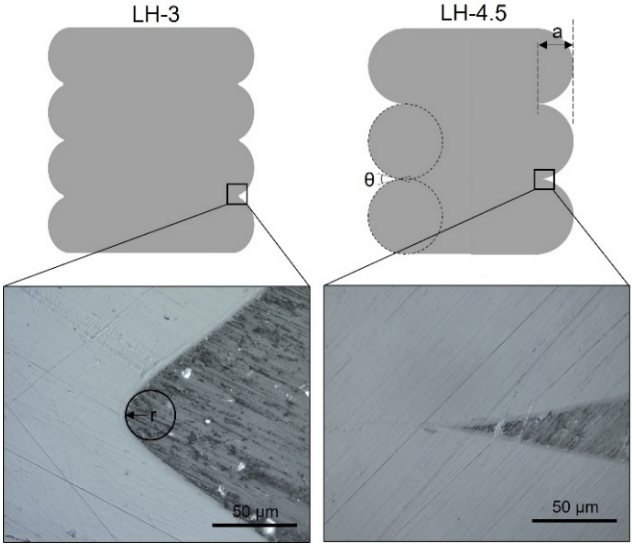

Fig. 7. Cross-sectional views of the interface notches show a rounded notch root for LH-3, while a crack-like root is observed for LH-4.5

Table 3.
Notch characteristics parameters

	Notch angle, θ, °	Notch depth, a, mm	Root radius, r, μm	Number of measurements
LH-3	47 ± 5	0.67 ± 0.03	22 ± 9	10
LH-4.5	25 ± 3	1.44 ± 0.04	-	10

Figure 8 shows a representative fractured sample from the LH-4.5 set. High-strain regions are present at multiple locations, causing the sample's damage to initiate at several points almost simultaneously. It results in the sample splitting into several parts after fracture, as shown in Figure 8. Additionally, the crack propagates in different directions, indicating that there is no preferred interface area for crack propagation.

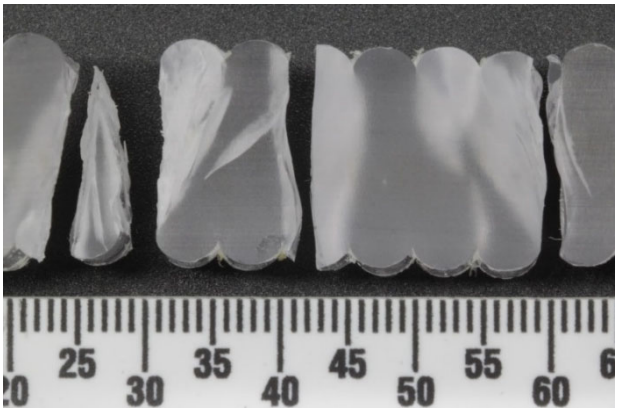

Fig. 8. LH-4.5 sample after fracture. Damage occurs at various locations due to the presence of high-strain regions between all filaments

The results of this study highlight a trade-off between print productivity and mechanical performance. Increasing the layer height enhances the deposition rate and printing efficiency; however, it also increases the severity of interface notches and may raise the void content due to a more rounded extrudate shape in bulk parts. At the same time, slower cooling associated with larger layer heights could enhance interdiffusion of polymer chains at the interface, partially mitigating the negative mechanical effects. Therefore, optimising layer height for industrial applications requires considering both geometric factors and chain-diffusion-driven bonding to achieve a balance between performance and productivity.

4. Conclusions

The study examines the effect of interface notches created by extrudate geometry on the tensile properties of FGF-printed parts, with a focus on samples printed at two distinct layer heights. It was found that interface notches act as strain concentration zones, leading to a decrease in ultimate stress and inducing brittle behaviour. The effect was significantly more pronounced at the higher layer height, with a 32% and 29% decrease in ultimate stress and strain at break, respectively, for the sample with the larger layer height. DIC results revealed that the interfaces can withstand higher levels of nominal strain at lower layer heights, likely due to a less severe local strain concentration at the notch root. The interface notches in both cases were characterised, showing a U-shaped notch at the lower layer height, while the notch root for the larger layer height was sharper, resembling a crack.

Furthermore, the notch angle decreased, and the notch depth increased with layer height, indicating that notch severity increases as layer height rises. For future studies, notch characterisation could be expanded to include different filament extrudate sizes and layer print parameters to gain a deeper understanding of how process parameters affect interface notch characteristics and mitigate their negative impact on part performance. Additionally, DIC results from the side view of the samples could provide valuable information regarding the strain concentration level at the notch root, where failure is typically initiated. Lastly, post-processing techniques to remove these features could be beneficial for improving the mechanical performance of parts with simple geometries.

Authors contribution

Maryam Shokrollahi developed the theory, performed experiments, and analysed results – 55%. Adam Smith contributed to methodology and data analysis – 25%. Martine Dubé and Ilyass Tabiai supervised the work and provided revisions to the manuscript, 20%. All authors discussed the results and approved the final manuscript.

Research funding

The work was funded by the Natural Sciences and Engineering Research Council of Canada (NSERC) and the Research Centre for High Performance Polymer and Composite Systems (CREPEC).

Additional information

The work was presented at the Casablanca International Conference on Additive Manufacturing, 2025.

References

[1] A. Patel, M. Taufik, Extrusion-Based Technology in Additive Manufacturing: A Comprehensive Review, Arabian Journal for Science and Engineering 49 (2024) 1309-1342. DOI: https://doi.org/10.1007/s13369-022-07539-1

[2] A.D. Dobrzańska-Danikiewicz, A. Bączyk, A review of additive manufacturing technologies, Archives of Materials Science and Engineering 128/2 (2024) 68-85. DOI: https://doi.org/10.5604/01.3001.0054.8755

[3] A.L. Woern, J.M. Pearce, 3-D Printable Polymer Pelletizer Chopper for Fused Granular Fabrication-Based Additive Manufacturing, Inventions 3/4 (2018) 78. DOI: https://doi.org/10.3390/inventions3040078

[4] A. Alexandre, F.A. Cruz Sanchez, H. Boudaoud, M. Camargo, J.M. Pearce, Mechanical Properties of Direct Waste Printing of Polylactic Acid with Universal Pellets Extruder: Comparison to Fused Filament Fabrication on Open-Source Desktop Three-Dimensional Printers, 3D Printing and Additive Manufacturing 7/5 (2020) 237-247. DOI: https://doi.org/10.1089/3dp.2019.0195

[5] F. Pignatelli, G. Percoco, An application- and market-oriented review on large format additive manufacturing, focusing on polymer pellet-based 3D printing, Progress in Additive Manufacturing 7 (2022) 1363-1377. DOI: https://doi.org/10.1007/s40964-022-00309-3

[6] Krishnanand, M. Taufik, Development of a Pellet and Filament Form Integrated Multi-Material Additive Manufacturing Co-Extruder, Proceedings of the ASME 2021 International Mechanical Engineering Congress and Exposition, Volume 2A: Advanced Manufacturing, Virtual, Online, 2021, V02AT02A012. DOI: https://doi.org/10.1115/IMECE2021-71044

[7] Krishnanand, M. Taufik, Surface roughness investigation of 3D printed parts via in-situ pellet-filament co-extrusion process, Materials and Manufacturing Processes 40/8 (2025) 1029-1048. DOI: https://doi.org/10.1080/10426914.2025.2487275

[8] M. Othmani, K. Zarbane, A. Chouaf, Effect of infill and density pattern on the mechanical behaviour of ABS parts manufactured by FDM using Taguchi and ANOVA approach, Archives of Materials Science and Engineering 111/2 (2021) 66-77. DOI: https://doi.org/10.5604/01.3001.0015.5806

[9] O. Aourik, M. Othmani, A. Chouaf, Experimental study of the fracture of CT specimens printed in PLA as a function of the raster width, Archives of Materials Science and Engineering 122/2 (2023) 78-85. DOI: https://doi.org/10.5604/01.3001.0053.9595

[10] A.D. Dobrzańska-Danikiewicz, B. Siwczyk, A. Bączyk, A. Romankiewicz, Mechanical properties of recycled PLA and PETG printed by FDM/FFM method, Journal of Achievements in Materials and Manufacturing Engineering 119/2 (2023) 49-59. DOI: https://doi.org/10.5604/01.3001.0053.9490

[11] M. Mrówka, M. Szymiczek, J. Lenża, Thermoplastic polyurethanes for mining application processing by 3D printing, Journal of Achievements in Materials and Manufacturing Engineering 95/1 (2019) 13-19. DOI: https://doi.org/10.5604/01.3001.0013.7620

[12] N.H. Patadiya, H.K. Dave, S.R. Rajpurohit, Effect of Build Orientation on Mechanical Strength of FDM Printed PLA, in: M.S. Shunmugam, M. Kanthababu (eds), Advances in Additive Manufacturing and Joining, Lecture Notes on Multidisciplinary Industrial Engineering, Springer, Singapore, 2020, 301-307. DOI: https://doi.org/10.1007/978-981-32-9433-2_26

[13] S.A. Tronvoll, N.P. Vedvik, C.W. Elverum, T. Welo, A new method for assessing anisotropy in fused deposition modeled parts using computed tomography data, The International Journal of Advanced Manufacturing Technology 105 (2019) 47-65. DOI: https://doi.org/10.1007/s00170-019-04081-7

[14] E. Barocio, B. Brenken, A. Favaloro, R.B. Pipes, Interlayer fusion bonding of semi-crystalline polymer composites in extrusion deposition additive manufacturing, Composites Science and Technology 230/2 (2022) 109334. DOI: https://doi.org/10.1016/j.compscitech.2022.109334

[15] H. Li, T. Wang, J. Sun, Z. Yu, The effect of process parameters in fused deposition modelling on bonding degree and mechanical properties, Rapid Prototyping Journal 24/1 (2018) 80-92. DOI: https://doi.org/10.1108/RPJ-06-2016-0090

[16] E. Brancewicz-Steinmetz, R. Valverde Vergara, V.H. Buzalski, J. Sawicki, Study of the adhesion between TPU and PLA in multi-material 3D printing, Journal of Achievements in Materials and Manufacturing Engineering 115/2 (2022) 49-56. DOI: https://doi.org/10.5604/01.3001.0016.2672

[17] J. Ghorbani, P. Koirala, Y.-L. Shen, M. Tehrani, Eliminating voids and reducing mechanical anisotropy

in fused filament fabrication parts by adjusting the filament extrusion rate, Journal of Manufacturing Processes 80 (2022) 651-658.
DOI: https://doi.org/10.1016/j.jmapro.2022.06.026
[18] T. Webbe Kerekes, H. Lim, W.Y. Joe, G.J. Yun, Characterization of process–deformation/damage property relationship of fused deposition modeling (FDM) 3D-printed specimens, Additive Manufacturing 25 (2019) 532-544.
DOI: https://doi.org/10.1016/j.addma.2018.11.008
[19] M. Shokrollahi, A.W. Smith, A. Levy, M. Dubé, I. Tabiai, Reassessing anisotropy in 3D printed structures: The role of extrudate geometry vs interface bonding, Journal of Manufacturing Processes 149 (2025) 456-472. DOI: https://doi.org/10.1016/j.jmapro.2025.05.070
[20] J. Allum, A. Moetazedian, A. Gleadall, V.V. Silberschmidt, Interlayer bonding has bulk-material strength in extrusion additive manufacturing: New understanding of anisotropy, Additive Manufacturing 34 (2020) 101297.
DOI: https://doi.org/10.1016/j.addma.2020.101297
[21] J. Allum, A. Gleadall, V.V. Silberschmidt, Fracture of 3D-printed micro-tensile specimens: filament-scale geometry-induced anisotropy, Procedia Structural Integrity 28 (2020) 591-601.
DOI: https://doi.org/10.1016/j.prostr.2020.10.069
[22] S. Kundurthi, F. Tran, S. Chen, J. Mapkar, M. Haq, Bead geometry–induced stress concentration factors in material extrusion polymer additive manufacturing, Rapid Prototyping Journal 29/7 (2023) 1438-1452. DOI: https://doi.org/10.1108/RPJ-11-2022-0404
[23] M.A. Sutton, J.J. Orteu, H. Schreier, Image Correlation for Shape, Motion and Deformation Measurements: Basic Concepts, Theory and Applications, Springer, New York, NY, USA, 2009.
DOI: https://doi.org/10.1007/978-0-387-78747-3